J. Mater. Environ. Sci. 7 (7) (2016) 2277-2287
ISSN : 2028-2508
CODEN: JMESC

Radio-frequency magnetron sputtering: a versatile tool for CdSe quantum dots depositions with controlled properties

A. Dahi[1,2*], P. Colson[3], C. Jamin[3], R. Cloots[3], M. Lismont[1], L. Dreesen[1*]

[1] *GRASP-Biophotonics, University of Liège, Institute of Physics B5a, Allée du 6 Août 17, B-4000 Liège, Belgium*
[2] *URCOM, EA 3221, FR CNRS 3038, Université du Havre, 25 rue Philippe Lebon, B.P. 540, 76058 Le Havre cedex, France*
[3] *GREEnMat-LCIS, University of Liège, Institute of Chemistry B6, Allée de la Chimie 3, B-4000 Liège, Belgium*

Received 08 Dec 2015, Revised 08 May 2016, Accepted 12 May 2016
**Corresponding author. E-mail: dahi_abdellatif@yahoo.fr (A. Dahi), Laurent.Dreesen@ulg.ac.be (L. Dreesen).*

Abstract

CdSe nanoparticles are of great interest for many applications. However, their size, shape, and aggregation are still difficult to control by the conventional synthesis methods. Here, we report on the synthesis of CdSe quantum dots (QDs), with an average diameter less than 10 nm, using radio-frequency magnetron sputtering (RFMS) on glass and silicon substrates at 25 °C. First, results show that a target-substrate distance of 13.5 cm and a chamber pressure of $2.2 .10^{-1}$ mbar were required to deposit a CdSe QDs layer on the substrates. The morphology and optical properties of CdSe QDs were then studied as a function of RF power and deposition time. The size of CdSe QDs increases with increasing both the RF power and the deposition time. UV-visible spectroscopy shows that the CdSe QDs layer deposited on the glass-substrate by RFMS has almost the same optical properties as the one obtained from commercial CdSe QDs solutions. In both cases, a shift of the characteristic absorption band of CdSe QDs towards the higher wavenumbers is observed with the QDs size increase. AFM confirms the success of CdSe QDs layer deposition by RFMS: CdSe QDs with a mean diameter of 7.5 ± 2 nm were observed for a RF power of 14 W, a chamber pressure of $2.2 .10^{-1}$ mbar, a target-substrate distance of 13.5 cm and a deposition time of 7.5 min (optimal values). With these parameters, the coverage of the substrate by the nano-objects is estimated at 25-30 % of the overall surface.

Keywords: CdSe quantum dots; nanoparticles; radio-frequency magnetron sputtering; optical properties; morphological properties

1. Introduction

The recent development of nanotechnology, leading to the development of materials with nanometer-sized dimensions and attractive properties, has opened up new horizons for many applications in various fields such as electronics or medicine. In particular semiconductor quantum dots (QDs) have received considerable attention owing to their unusual electronic and optical properties [1-7]. QDs are semiconductor nanoparticles (NPs) characterized by very small dimensions (< 10 nm). This small size scale leads to large surface areas and unique size-related optical properties arising from quantum confinement [1]. For instance, narrow emission bands in a wide UV-visible spectral range can be obtained by an appropriate selection of the size, shape, and composition of QDs [8,9]. They have become more and more important in biosensing and imaging because they offer very attractive optical properties such as higher photoluminescence (PL) efficiency, higher photostability, and wider selections of excitation and emission wavelengths with respect to traditional fluorescence labels [8-12]. These advantages are of great interest for detection techniques such as fluorescence, fluorescence lifetime measurement, fluorescence resonance energy transfer (FRET) and multiphoton microscopy [13-15]. New fields of application are also currently under consideration: catalysis, semiconductors industry, pharmacology and biotechnologies [16-20].

In particular, II–VI semiconductor (CdSe, CdS, ZnO and ZnS) NPs attracted much attention due to their size-dependent photo- and electro-luminescence properties and promising applications in optoelectronics. For instance, CdSe has a wide optical band gap (1.74 eV), making it a suitable material for optical applications. When CdSe QDs are used instead of thin films, the optical gap can be tuned from deep red (1.7 eV) to green (2.4 eV) by simply reducing the nanoparticle diameter from 20 to 2 nm [21,22]. CdSe NPs can be used in various applications including laser diodes, high efficiency solar cells, nanosensing and biomedical imaging [21, 23-27].

To benefit from the specific properties of QDs, it is essential to control various key parameters such as their size, shape, specific surface area, surface density, etc. An extremely active and prolific field in nanomaterials is thus focused on finding appropriated deposition tools allowing the size and morphology controls of the NPs. QDs can be synthesized by many techniques, including sol-gel process, hydrothermal methods, sparking process, laser ablation, laser pyrolysis, spray deposition, MOCVD and RF induction plasma [28-35]. However, with most of them, the QDs size and shape as well as the coverage of the surface are difficult to control. Moreover, the chemical preparation methods, not friendly to the environment, require the use of precursors and/or solvents which can lead to contaminations of the deposited layer. In addition, stabilizing agents are often added in the solutions to prevent NPs aggregation, which has a significant impact on their optical properties as a result of size changes. These stabilizing agents generally also contaminate the NPs surface, making further functionalization difficult, especially when NPs need to be deposited on a substrate. All these reasons do not encourage potential industrial applications with the chemical methods. As regards the physical synthesis techniques (laser ablation and RF induction plasma), although environment-friendly, are not adapted to industry due to the small size of the produced samples. Moreover, most of the aforementioned synthesis methods give rise to powders of NPs, whereas NPs directly adsorbed on a surface are suitable for most applications. Therefore, further progress on applications of NPs essentially relies upon the development in powerful synthesis tools.

Physical vapor deposition (PVD) techniques such as radio-frequency magnetron sputtering (RFMS) overcome most of the aforementioned drawbacks. For example, precursors or solvents are not required due to the physical nature of the deposition process. The contamination of the surface is also reduced because high purity targets are used and the method is performed under vacuum. Moreover, the control of the sputtering conditions (pressure, temperature, deposition time) also allows the tuning of the size, shape and particle density (number of NPs/unit area) of NPs, and therefore of their optical properties [36]. PVD deposition techniques have been previously applied to the deposition of CdSe thin films and CdSe QDs embedded in SiO_2 or in an organic matrix [37-39]. Sharma et al. [40] have recently studied the structural, optical, and surface potential properties of CdSe NPs/ZnS thin-films. The CdSe NPs of varying diameters were prepared by controlling deposition time in magnetron sputtering deposition process. Subila et al. [41] have investigated the crystal-structure-dependent luminescence properties of CdSe QDs, and given precious data on the role of crystal structure and surface composition in the CdSe QDs properties. Recently, we reported on the synthesis of CdSe NPs on glass and silicon substrates by RFMS [42]. In that article, we compared the optical properties of CdSe QDs prepared by wet chemistry and RFMS with a precise set of experimental conditions. No detail was furnished on the effect of the sputtering parameters on the morphology and the optical properties of the deposited CdSe QDs layer. The goal of the present paper is to fill this lack because it was never dealt with before. The formation of CdSe QDs is therefore investigated under different sputtering conditions including RF power, argon pressure in the plasma chamber and deposition time. The samples are characterized for their morphological and optical properties by atomic force microscopy and UV-visible spectroscopy, respectively. For comparison, the CdSe QDs depositions were also performed by wet chemistry using commercial suspensions.

2. Experimental

2.1. *CdSe Quantum Dots deposition*

Two types of substrates were used to grow the CdSe QDs: glass substrate (Borosilicate) and silicon wafer (p-type; 001; ρ=4.6 Ω.cm). Glass and silicon substrates were used for UV-Vis absorbance measurements and for morphological characterization, respectively. All substrates were cut into 1×1 cm^2 size, pre-cleaned ultrasonically in acetone (purity ≥ 99 % ; VWR Prolabo) and then in ethanol (purity ≥ 99.5 % ; VWR Prolabo) for 15 min, and finally dried under pure nitrogen stream.

The CdSe QDs depositions were carried out by RFMS, which was driven by a 13.6 MHz generator (PFG 300 RF; Hüttinger). All depositions were performed at ambient temperature (23 ± 2 °C). After having fixed the substrate (Si or glass) on the substrate holder, the distance between the CdSe target (from Ampere Industrie (France), purity 99.99 %, diameter 33 mm, thickness 3 mm) and the substrate was set at 13.5 cm (this choice will be justified later). A dry primary pump (ACP Series; ADIXON) and a hybrid turbomolecular pump (Alcatel ATS 100) allowed obtaining a base pressure in the sputtering chamber reactor of 10^{-7} mbar. Mass flowmeters (FCU-4; VACOTEC) controlled the amount of injected argon gas (purity 99.99 %; Alphagaz). In order to define optimum conditions, three different parameters were tested: RF power (from 5 to 30 W), chamber pressure (from 1.1 10^{-1} to 4.5 10^{-1} mbar) and deposition time (from 7.5 to 15 min). The fresh treated substrates were characterized by UV-visible spectroscopy and AFM.

For the comparison, CdSe QDs depositions were also performed by wet chemistry using commercial suspensions. For this purpose, six kinds of CdSe QDs suspensions (Sigma-Aldrich, LumidotTM CdSe-6 quantum dot NPs kit [43]), with diameter ranging between 2.1 and 6.6 nm, were used. They are named L480, L520, L560, L590, L610 and L640 hereafter with respect to the wavelength of their fluorescence maximum, i.e.; 480, 520, 560, 593, 610 and 640 nm, respectively. In fact, each lumidot suspension shows a characteristic UV-Vis absorption band of CdSe QDs with a precise position depending on the QDs size [43]. The substrates (Si or glass) were immersed in a 10^{-3} M CdSe QDs commercial solution in toluene (purity ≥ 99 %; VWR Prolabo) during 18 h, then thoroughly rinsed with high purity water and dried under nitrogen flow.

2.2 *UV-Vis spectroscopy*

The UV-visible absorption spectra of the CdSe QDs layer deposited on the glass-substrates were recorded for wavelength between 400 and 850 nm using a multichannel spectrophotometer (Ocean optics, model QE65000FL). For the CdSe QDs suspensions, a cell with a 1 cm optical path was used.

2.3 *Atomic Force Microscopy*

The surface morphology was examined by atomic force microscopy using a NanoScope® IIIA (Digital Instruments – Veeco, Santa Barbara, CA, USA). The imaging process was performed in tapping (intermittent contact) mode in air at room temperature (23 ± 2 °C) using silicon cantilevers (SS-ISC-225C3.0/-/R model from Team Nanotec). They were characterized by a resonance frequency around 75 kHz, a nominal spring constant of 3.0 N/m and an apex radius of curvature of 5 nm. Average roughness (Ra) of the surface was obtained from AFM scans over surface areas of 0.5 µm x 0.5 µm, three times at a different location for each sample.

3. Results and discussion

3.1. *UV-Vis absorption of commercial CdSe QDs*

All UV-visible absorption spectra of the commercial CdSe QDs suspensions show a characteristic absorption band of CdSe QDs that varies between 440 and 640 nm [43], depending on the QDs size. For each solution, this band reveals the presence of QDs with a monodisperse size distribution. Knowing the size of the commercial CdSe QDs (data provided by the manufacturer), we have represented in Figure 1 the wavelength of the characteristic absorption band of CdSe QDs (see the wavelength values in the experimental section) as a function of QDs size. It can be clearly seen that the characteristic absorption band of CdSe QDs shifts towards the higher wavenumbers with the increase of QDs size. The same result was obtained by Murray et al. who studied the synthesis and characterization of nearly monodisperse CdSe semiconductor nanocrystallites [22]. The QD-size-dependent shift in the absorption band position is attributed to quantum confinement effects [13,22,44-46]. Indeed, the quantum confinement effect, occurring in nanometer-sized semiconductors, widens their band gap and generates well-defined energy levels at the band edges. This causes a redshift in the threshold absorption wavelength with increasing particle size and induces luminescence which is strictly correlated to particle size. Therefore, the position of the absorption (as well as the luminescence peaks) can be fine-tuned by controlling the particle diameter and the size distribution during manufacturing, in order to create a large group of "fluorophores" with precise optical properties on the surface [13].

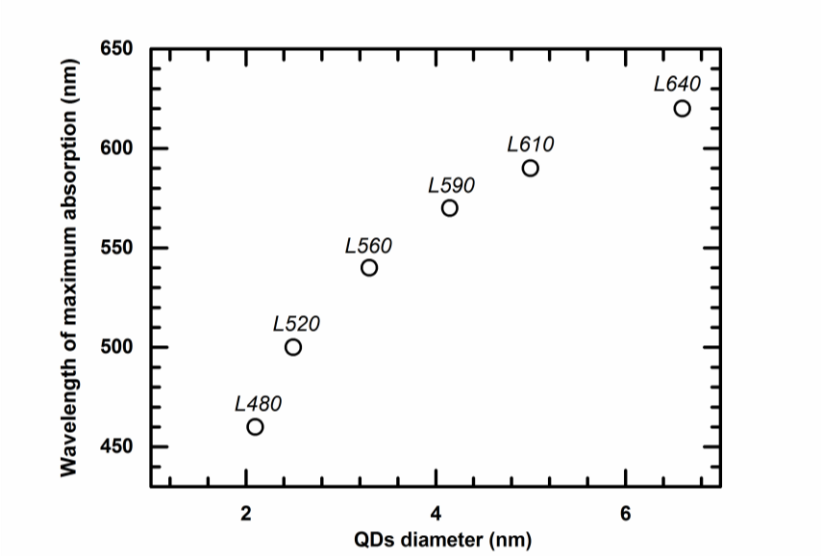

Figure 1. Wavelengths of the characteristic absorption band of the commercial CdSe QDs as a function of their diameter. The labels meaning has been introduced in the experimental section of the manuscript, the number highlighting the wavelength of maximum fluorescence.

To compare the absorption properties of the commercials CdSe QDs either in solution or deposited on a glass surface, glass substrates were wetted by the commercial CdSe QDs suspensions. After evaporation of the solvent, the absorption spectra of various depositions of CdSe QDs have been recorded (Figure 2).

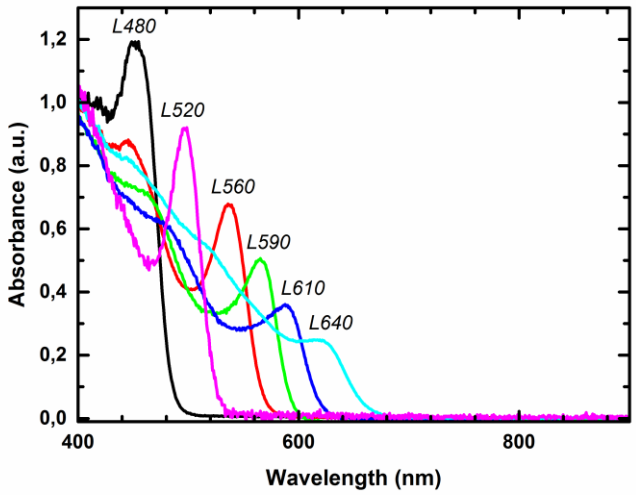

Figure 2. UV-visible absorption spectra of the commercial CdSe QDs suspensions coated on glass substrates (measurements carried out after evaporation of the solvent). All spectra are normalized by the absorbance value at 400 nm. The labels meaning has been introduced in the experimental section of the manuscript, the number highlighting the wavelength of maximum fluorescence.

Results show that the positions of the characteristic absorption bands of the commercial CdSe QDs deposited on a glass surface are 3-4% lower than that of the commercial CdSe QDs in suspension (see the wavelength values for L480, L520, L560, L590, L610 and L640 in the experimental section). This means that the position of the characteristic absorption band of CdSe QDs is almost independent of the QDs environment (either in solution or coated on a surface). On the other hand, the presence of a well-defined band on all absorption

spectra suggests the coating of the glass-substrate by non-aggregated CdSe QDs having a monodisperse size distribution [22] (a necessary condition for the appearance of the characteristic absorption band of CdSe QDs). Our objective was thus to reproduce the absorption spectra of Figure 2 using radio-frequency magnetron sputtering (RFMS). By the way, we will avoid the use of the hexadecylamine capping molecules which prevent surface functionalization as previously mentioned [42].

3.2. *UV-Vis absorption of CdSe QDs coated by RFMS*

At fixed deposition temperature (25 °C), the parameters affecting the deposition by RFMS are the RF power (P), the argon pressure (p), the target-substrate distance (d) and the deposition time (t). To fabricate CdSe QDs on the substrates by RFMS, it was necessary to reduce the deposition speed. Two ways were used to do that. First, as regards the target-substrate distance, the longer the distance is, the higher is the number of collisions between the sputtered atoms and the plasma species, and the lower is the deposition speed [47]. Therefore, we fixed the target-substrate distance at 13.5 cm, knowing that in our case the available longest distance is 15 cm. Second, a high argon pressure in the order of 10^{-1} mbar was a necessary condition to reduce the deposition speed and, consequently, to deposit CdSe QDs on the substrates. In fact, the pressure affects especially the number of collisions between the sputtered atoms and the plasma species during the transfer of target atoms toward the substrate. As a result, the collisions lower the energy of the sputtered atoms and change their trajectory. In other words, the higher the number of collisions (with high chamber pressure), the longer is the mean free path of the sputtered atoms, and the lower is the deposition speed. Figure 3 shows UV-visible absorption spectra of CdSe QDs coated on the glass substrates by RFMS at three different chamber pressures: 1.1 10^{-1}, 2.2 10^{-1} and 4.5 10^{-1} mbar. This last value is the highest possible pressure with our set-up. The UV-visible absorption spectra of the sample prepared by RFMS at 2.2 10^{-1} mbar is the only one showing a characteristic absorption band of CdSe QDs, indicated by an arrow, with a maximum at 655 nm (see the curve B in Figure 3). This feature lies in the same spectral region as the ones observed with commercial CdSe QDs deposited on the glass substrates (i.e. 440-660 nm, see Figure 2).

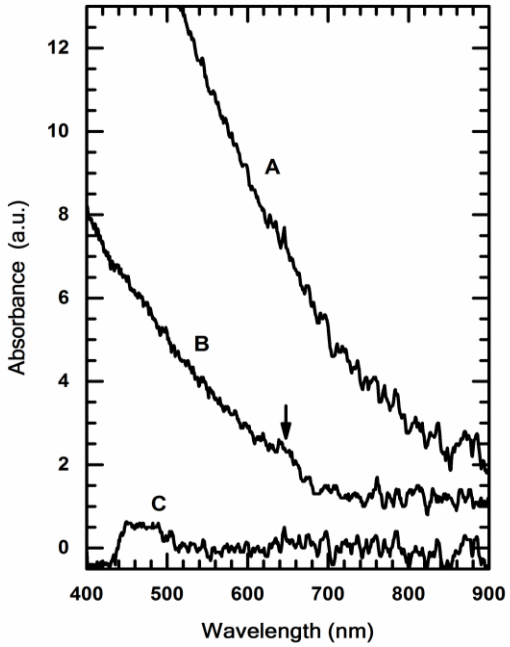

Figure 3. UV-visible absorption spectra of CdSe QDs deposited on glass substrates by RFMS as function of the pressure chamber: 1.1 10^{-1} mbar (A), 2.2 10^{-1} mbar (B) and 4.5 10^{-1} mbar (C). A and B curves are shifted by 2 and 1, respectively. The sputtering power, deposition time and target-substrate distance were 14 W, 7.5 min and 13.5 cm, respectively.

The success of CdSe QDs layer deposition by RFMS at 2.2 10^{-1} mbar is therefore confirmed. The increase of the chamber pressure from 2.2 10^{-1} to 4.5 10^{-1} mbar prevent deposition. Indeed, the absorption is close to zero for the sample prepared by RFMS at 4.5 10^{-1} mbar (see the curve C in Figure 3). With this chamber pressure, the plasma species constitutes a barrier preventing the sputtered atoms from reaching the substrate. At a pressure equal to 1.1 10^{-1} mbar, the fabricated sample is characterized by a strong absorbance and the absence of the characteristic absorption band of CdSe QDs (see the curve A in Figure 3), suggesting a thin-film deposition. After the deposition, a clearly visible dark brown colour over the entire glass surface confirms the formation of a thin-film deposition.

Having set the target-substrate distance at 13.5 cm and the chamber pressure at 2.2 10^{-1} mbar, we have performed several coatings by changing the value of one parameter (either the RF power or the deposition time) while the other was kept constant. Figures 4a and 4b show the UV-visible absorption spectra of the CdSe QDs deposited on the glass-substrate by RFMS with the different conditions summarized in Table 1. The absorption spectra of the samples A, B, C and D show a characteristic absorption band of CdSe QDs, indicated by arrows, with maximum at 610, 612, 623 and 655 nm, respectively. These bands are almost located in the same spectral region that the absorption bands of commercial CdSe QDs deposited on the glass substrate (i.e. 440-660 nm, see Figure 2). This means that NPs with a controlled size distribution are deposited on the glass-substrate by RFMS under the sputtering conditions of A, B, C and D samples. The number of CdSe QDs deposited by RFMS is probably weaker than the one associated to layers deposited on the glass-substrate using commercial CdSe QDs solutions, which explains the low intensity of the bands in the former case and a lower signal to noise ratio. On the other hand, it is also important to notice that the state or nature of CdSe QDs deposited by RFMS is slightly different from those of CdSe QDs deposited from the commercial solutions. In fact, the commercial CdSe QDs are of core-shell type, *i.e.*, they have a core in CdSe and a protective layer from ligands to prevent aggregation. This involves a slight change in the absorption spectrum compared to the one of pure CdSe QDs.

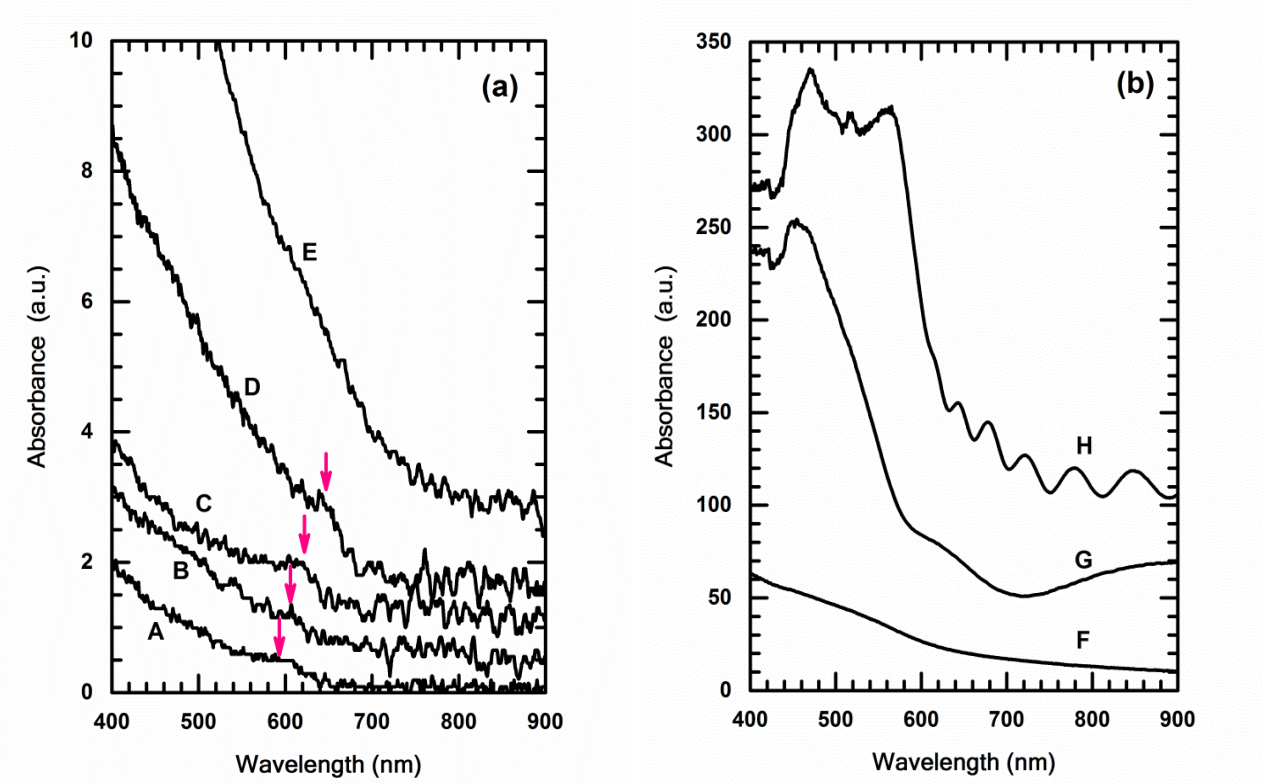

Figure 4. UV-visible absorption spectra of the CdSe QDs deposited on glass substrates by RFMS under the sputtering conditions described in Table 1. Spectra B, C, D, E, G and H are respectively shifted by 0.5, 1, 1.5, 2, 50 and 100, respectively. The arbitrary units are the same for both figures.

Table 1. RFMS deposition conditions of the CdSe QDs on the substrates (Si and glass). The chamber pressure and the distance target-substrate were 2.2 10^{-1} mbar and 13.5 cm, respectively.

Sample	A	B	C	D	E	F	G	H
P (W)	5	5	5	14	14	20	25	30
t (min)	7.5	9.25	11	7.5	15	7.5	7.5	7.5

At low RF power (5 W) and deposition time equal to 7.5 min (*i.e.* sample A (Table 1)), the absorbance is very low (Figure 4, curve A) and suggests a deposition of CdSe QDs with the lowest diameter value. The characteristic absorption band of CdSe QDs (at ~ 600 nm) is barely visible. A progressive increase of the deposition time involves an increase in absorbance, associated with a slight shift of the characteristic absorption band of CdSe QDs towards the higher wavenumbers (Figure 4, curves B and C). The characteristic absorption band of CdSe QDs is also more clearly visible under the sputtering conditions of the sample C. All these observations highlight a gradual growth in the size of CdSe QDs with rising deposition time, and possibly an increase of their number on the substrate surface. This is in accordance with the study of Kumar et al. [48] on the growth of NPs from the sputtering of a tungsten cathode in DC argon glow discharges. They indicated that for longer discharge durations, the tungsten primary particles (~ 30 nm) agglomerate to form bigger NPs (80-150 nm). This is also in keeping with Sharma et al. who investigated the properties of CdSe nanoparticles (NPs) prepared on ZnS thin-films [40]. Indeed, CdSe NPs of varying sizes were prepared by controlling deposition time in magnetron sputter deposition process. They observed an increase in the size of CdSe NPs from 5 nm for 10 s, 7 nm for 30 s and 10 nm for 50 s, and showed that the coverage of the ZnS films with CdSe nanoparticles increases when the deposition time of CdSe NPs increases. By increasing the RF power from 5 to 14 W, the absorbance increases significantly (Figure 4, curves D and E) due to the generation of a larger number of photo-carriers that contribute to the emission cross section [45]. In fact, the increase in RF power increases the concentration of injected CdSe particles, and therefore increases the NPs surface density. In the other hand, in the case of the sample D, the characteristic absorption band of CdSe QDs (Figure 4, curve D) shifts more towards the higher wavenumbers (redshift) with the increase in RF power (exactly at 655 nm). This indicates an increase of the QDs diameter with the RF power, as highlighted at the beginning of the R&D section. Indeed, the energy of the sputtered atoms increases with RF power, which has the consequence of forming particles or aggregates of larger size [45] as we will see in the AFM section. Always at the same power value of 14 W, the increase of the deposition time from 7.5 to 15 min (*i.e.* sample) implies both an increase in absorbance and the disappearance of the characteristic absorption band of CdSe QDs. The same goes for the depositions performed at a RF power of 20, 25 and 30 W (see Figure 4b): strong increase in absorbance and absence of the characteristic absorption band of CdSe QDs. The disappearance of the characteristic absorption band of CdSe QDs may be due to a polydisperse size distribution or, more probably, the formation of a continuous thin-film of CdSe on the surface. A clearly visible dark brown colour over the entire glass surface was observed in the last cases (*i.e.* the samples F, G and H (Figure 4b)), and suggests the formation of a thin-film deposition. The oscillations in the absorbance signal, observed on the spectra G and H (Figure 4b), are due to interference phenomena. In conclusion, the size of CdSe QDs increases with increasing either the power or the deposition time, until to reach thresholds. This growth in the size of CdSe QDs is highlighted by the shift of the characteristic absorption band of CdSe QDs towards the higher wavenumbers on the absorption spectra, as previously observed in Figure 1 with the commercial CdSe QDs suspensions. Since the characteristic bands of QDs are more clearly visible under the conditions of the samples C and D, we analyzed more closely these two samples by AFM. Let us also mention that we also performed depositions at a RF power of 10 W (not shown). In these conditions, a slight increase in absorbance was noted compared to the depositions at 5 W, but no clear absorption band characteristic of CdSe QDs was observed.

3.4. *AFM Analysis*

Figure 5 shows the 2D and 3D AFM images of the Si substrate surface before and after the deposition of the CdSe QDs by RFMS under the sputtering conditions of the samples C and D. The surface roughness for a neat Si sample, samples C and D are reported on Table 2. Figure 5a shows the AFM image of the neat Si substrate (before deposition). Its surface root-mean-square roughness, defined as the average height deviations taken from the mean plane, is equal to 0.07 nm. After RFMS deposition, and irrespective of the sputtering conditions (sample C or D), the substrate surface becomes completely coated by a layer of dome-shaped CdSe NPs having a diameter less than 10 nm (see the 2D AFM images in Figure 5). From theses 2D images, the deposition is far from being considered as a continuous film. Under the preparation conditions of sample C, although the CdSe QDs are well nanometer-size particles, it is difficult to distinguish particles of controlled size on the surface (Figure 5b). The surface roughness increases from 0.07 nm for the neat substrate to 0.16 nm for the sample C. In addition, the degree of size uniformity of the sample C is weak compared to the one of sample D. Consequently, it is difficult to determine the mean diameter of the CdSe QDs prepared under the sputtering conditions of the sample C.

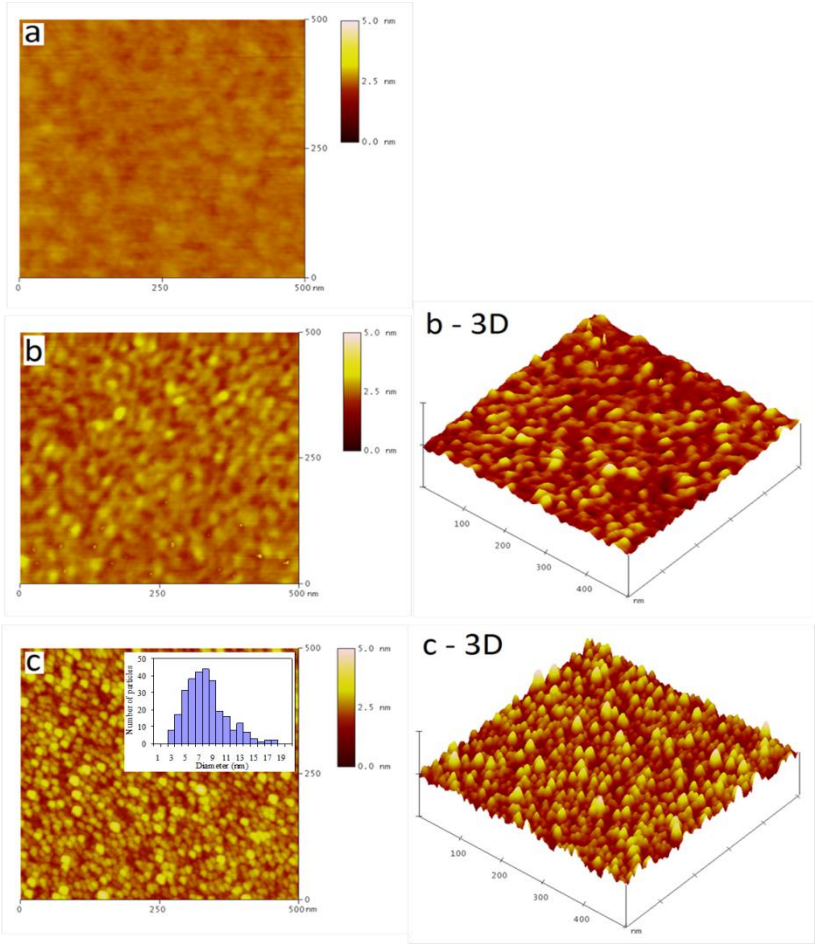

Figure 5: 2D and 3D AFM images of the Si substrate surface before and after the deposition of CdSe QDs by RFMS under the sputtering conditions of the samples C and D: (a) bare substrate, (b) sample C and (c) sample D. Inset in (c) is a histogram of the size distribution of the CdSe NPs.

All these observations suggest that most of CdSe QDs of the sample C are not yet fully mature. By contrast, when the RF power is increased to 15 W and the deposition time is reduced to 7.5 min (the sputtering conditions of the sample D), Figure 5c shows a homogenous coverage of the surface by circular QDs of a well-defined size. The histogram of particle size distribution of the samples D is shown as inset in Figure 5c, and

shows a size distribution ranging between 4 and 11 nm with a mean diameter of 7.5 ± 2 nm, after tip-size deconvolution [49]. This diameter value is in good agreement with the one (~ 7 nm) associated to layer deposited on the glass-substrate using L640 as commercial solution (see Figure 1). This result demonstrates that we can deposit QDs by magnetron sputtering system with almost the same optical properties (same size) than the ones obtained by wet chemistry. Figure 6 highlights this comparison. This also agrees with the results of Murray et al. showing an absorption band at 650 nm for CdSe nanocrystallites of 8.3 nm diameter [22], although their synthesis method was different from ours. The surface roughness increases from 0.07 nm for the neat substrate to 0.30 nm for the sample D. The roughness variation is significant and is expected because the QDs distribution has a regular pattern, as evidenced by the 3D AFM image (Figure 5c). Using a standard image analysis program (Image J), we evaluated for the sample D the coverage of the surface by the QDs at 25-30 % of the overall surface. From the 2D and 3D AFM images of samples, it is clear that the sample D exhibits well-resolved regular topography of CdSe QDs with nanometer-size diameter. Moreover, the colour contrast of the AFM image of the sample D is higher than the one associated to sample C suggesting that the CdSe QDs growth under the conditions of the sample D reached an advanced state in maturation. In conclusion, the most interesting CdSe QDs features appear with the sample D sputtering conditions. This result confirms what was mentioned in the UV-Vis spectroscopy section: the increase in RF power (from 5 to 14 W) induces the formation of mature and bigger QDs, involving a shift of the characteristic absorption band of CdSe QDs towards the higher wavenumbers. Undoubtedly, the increase of the RF power leads to a high degree of intermixing via diffusion [45,47]. This favors nucleation on subsequent QDs. At a higher RF power (sample D), the CdSe ad-atoms are expected to diffuse to a longer distance on the surface and prefer to produce new nucleation centers. In conclusion, the plasma parameters used for sample D seem to offer the most scope for practically implementing a deposition of mature CdSe QDs finely distributed on the substrate surface, and whose size and optical properties are tailored.

Table 2: Average roughness (Ra) of bare Si substrate, sample C and sample D.

	Bare substrate	Sample C	Sample D
Ra (nm)	0.07	0.16	0.30

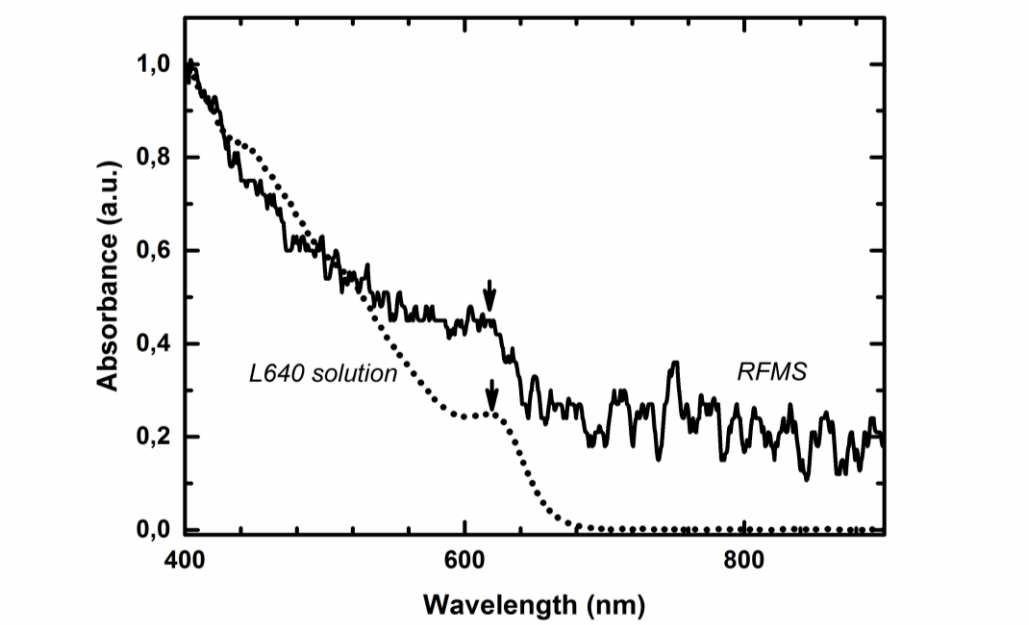

Figure 6: Comparison of sample produced by RFMS and from commercial L640 solution. Both spectra exhibit a characteristic absorption band of CdSe QDs in the same region.

Conclusions

We synthesized CdSe QDs with controlled size and shape using RFMS technique at 25 °C. This tool enables to well control the size and shape of QDs, unlike to the conventional synthesis methods. A target-substrate distance of 13.5 cm and a chamber pressure of 2.2 10^{-1} mbar were the first required parameters to deposit a CdSe QDs layer on the substrates by RFMS. Increasing the RF power and the deposition time resulted in an increase of the size of CdSe QDs. The optimal values for the RF power and the deposition time were 14 W and 7.5 min, respectively. In this case, the mean diameter of CdSe QDs was 7.5 ± 2 nm, with a size distribution ranging between 4 to 11 nm. The CdSe QDs prepared by RFMS exhibited optical properties similar to those obtained using commercial suspensions either in solution or deposited on the surface.

Acknowledgments-This work was supported by the "Fonds de la Recherche Scientifique – FRS" (Project N° 2.4504.12) and the University of Liège (Projects N° D-11/10 and FSRC-14/03). We thank Prof. Rudi Cloots for the access to AFM facilities (University of Liege - Microscopy Research and Teaching Support Unit (CAREμ)).

References

1. Jacak L., Hawrylak P., Wojs A., Quantum Dots Springer-Verlag, Berlin, 1998.
2. Banyai L. B., Koch S. W., Semiconductor Quantum Dots, World Scientific, Singapore, 1993.
3. Yoffe A. D., *Adv. Phys.* 42 (1993) 173.
4. Woggon U., Optical Properties of Quantum Dots, Springer-Verlag, Berlin, 1996.
5. Chakraborty T., Quantum Dots: A Survey of the Properties of Artificial Atoms, Elsevier, Amsterdam, 1999.
6. Harrison P., Quantum Wells, Wires, and Dots, Wiley, New York, 2000.
7. Efros Al. L., Rosen M., *Annu. Rev. Mater. Sci.* 30 (2000) 475.
8. Ruan G., Agrawal A., Smith A. M., Gao X., Nie S., *Rev. Fluoresc.* 3 (2006) 181.
9. Gao X., Yang L., Petros J. A., Marshall F. F., Simons J. W., Nie S., *Curr. Opin. Biotechnol.* 16 (2005) 63.
10. Smith A. M., Nie S., *Analyst* 129 (2004) 672.
11. Klostranec J. M., Chan W. C. W., *Adv. Mater.* 18 (2006) 195.
12. Biju V., Itoh T., Anas A., Sujith A., Ishikawa M., *Anal. Bioanal. Chem.* 391 (2008) 2469.
13. Zhong W., *Anal. Bioanal. Chem.* 394 (2009) 47.
14. Algar W. R., Krull U. J., *Anal. Bioanal. Chem.* 391 (2008) 1609.
15. Resch-Genger U., Grabolle M., Cavaliere-Jaricot S., Nitschke R., Nann T., *Nat. Methods* 5 (2008) 763.
16. Michalet X., Pinaud F.F., Bentolila L.A., Tsay J.M., Doose S., Li J.J., Sundaresan G., Wu A.M., Gambhir S.S., Weiss S., *Science* 307 (2005) 538.
17. Juzenas P., Chen W., Sun Y.-P., Coelho M.A.N., Generalov R., Generalova N., Christensen I. L., *Adv. Drug Delivery Rev.* 60 (2008) 1600.
18. Lu Y., Liu J., *Wiley Interdiscip. Rev. Nanomed. Nanobiotechnol.* 1 (2009) 35.
19. Dai Q., Duty C. E., Hu M. Z., *Small* 6 (2010) 1577.
20. Zrazhevskiv P., Sena M., Gao X., *Chem. Soc. Rev.* 39 (2010) 4326.
21. Alivisatos A. P., *Science* 271 (1996) 933.
22. Murray C. B., Norris D. J., Bawendi M. G., *J. Am. Chem. Soc.* 115 (1993) 8706.
23. Ma C., Ding Y., Moore D., Wang X., Wang Z. L., *J. Am. Chem. Soc.* 126 (2004) 708.
24. Gal D., Hodes G., Hariskos D., Braunger D., Schock H.-W., *Appl. Phys. Lett.* 73 (1998) 3135.
25. M. Califano, A. Zunger, A. Franceschetti, Appl. Phys. Lett. 84 (2004) 2409.
26. Hendry E., Koeberg M., Wang F., Zhang H., De Mello Donega C., Vanmaekelberg D., Bonn M., *Phys. Rev. Lett.* 96 (2006) 057408.
27. Sholin V., Breeze A. J., Anderson I. E., Sahoo Y., Reddy D., Carter S.A., *Sol. Energy Mater. Sol. Cells* 92 (2008) 1706.
28. Schneider M., Baiker J., *J. Mater. Chem.* 2 (1992) 587.

29. Cheng C., Ma J., Zhao Z., Qi L., *Chem. Mater.* 7 (1995) 663.
30. Sun Y., Li A., Qi M., Zhang L., Yao X., *Mater. Sci. Eng. B* 86 (2001) 185.
31. Seto T., Kawakami Y., Suzuki N., Hirasawa M., Kano S., Aya N., Sasaki S., Shimura H., *J. Nanoparticles Res.* 3 (2001) 185.
32. Thongsuwan W., Kumpika T., Singjai P., *Curr. Appl. Phys.* 8 (2007) 563.
33. Figgemeier E., Kylberg W., Constable E., Scarisoreanu M., Alexandrescu R., Morjan I., Soare I., Birjega R., Opovici E., Fleaca C., Gavrila-Florescu L., Prodan G., *Appl. Surf. Sci.* 254 (2007) 1037.
34. Ranga Rao A., Dutta V., *Sol. Energ. Mater. Sol. Cell.* 91 (2007) 1075.
35. Li J.-G., Ikeda M., Moriyoshi Y., Ishigaki T., *J. Phys. D: Appl. Phys* 40 (2007) 2348.
36. Dreesen L., Cecchet F., Lucas S., *Plasma Process. Polym.* 6 (2009) S849.
37. Babu Dayal P., Rama Rao N. V., Mehta B. R., Shivaprasad S. M., Paulson P. D., *Materials Research Society Symposium – Proceedings* 789 (2003) 3.
38. Levichev S., Chahboun A., AG Rolo A. G., Conde O, Gomes MJM, *Thin Solid Films* 517 (2009) 2538.
39. Campos-Gonzalez E., Rodriguez-Fragoso P., Gonzalez de la Cruz G., Santoyo-Salazar J., Zelaya-Angel O., *J. Cryst. Growth* 338 (2012) 251.
40. Sharma I., Batra Y., Mehta B. R., *J. Appl. Phys.* 117 (2015) 245310.
41. Subila K. B., Kishore Kumar G., Shivaprasad S. M., George Thomas K., *J. Phys. Chem. Lett.* 4 (2013) 2774.
42. Humbert C., Dahi A., Dalstein L., Busson B., Lismont M., Dreesen L., *J. Coll. Int. Sci.* 445 (2015) 69.
43. http://www.sigmaaldrich.com/catalog/product/aldrich/662550?lang=en&region=MA
44. Choi S.-H., Song H., Park I. K., Yum J.-H., Kim S.-S., Lee S., Sung Y.-E., *J. Photoch. Photobio. A* 179 (2006) 135.
45. Samavati A., Othaman Z., Ghoshal S. K., Dousti M. R. A., *Int. J. Mol. Sci.* 13 (2012) 12880.
46. Banerjee A. N., Joo S. X., Min B.-K., *J. Appl. Phys.* 112 (2012) 114329.
47. Asanithi P., Chaiyakun S., Limsuwan P., *J. Nanomater.* 2012 (2012) Article ID 963609.
48. Kishor Kumar K., Couëdel L., Arnas C., *Phys. Plasmas* 20 (2013) 043707.
49. Rasa M., Kuipers B. W. M., Philipse A. P., *J. Colloid Interf. Sci.* 250 (2002) 303.